

Alkaline Phosphatase ALPPL-2 Is a Novel Pancreatic Carcinoma-Associated Protein

Pooja Dua^{1,3}, Hye Suk Kang³, Seung-Mo Hong², Ming-Sound Tsao⁴, Soyoun Kim¹, and Dong-ki Lee³

Abstract

Pancreatic ductal adenocarcinoma (PDAC) is a highly aggressive malignancy with a very low median survival rate. The lack of early sensitive diagnostic markers is one of the main causes of PDAC-associated lethality. Therefore, to identify novel pancreatic cancer biomarkers that can facilitate early diagnosis and also help in the development of effective therapeutics, we developed RNA aptamers targeting pancreatic cancer by Cell-systematic evolution of ligands by exponential enrichment (SELEX) approach. Using a selection strategy that could generate aptamers for 2 pancreatic cancer cell lines in one selection scheme, we identified an aptamer SQ-2 that could recognize pancreatic cancer cells with high specificity. Next, by applying 2 alternative approaches: (i) aptamer-based target pull-down and (ii) genome-wide microarray-based identification of differentially expressed mRNAs in aptamer-positive and -negative cells, we identified alkaline phosphatase placental-like 2 (ALPPL-2), an oncofetal protein, as the target of SQ-2. ALPPL-2 was found to be ectopically expressed in many pancreatic cancer cell lines at both mRNA and protein levels. RNA interference-mediated ALPPL-2 knockdown identified novel tumor-associated functions of this protein in pancreatic cancer cell growth and invasion. In addition, the aptamer-mediated identification of ALPPL-2 on the cell surface and cell secretions of pancreatic cancer cells supports its potential use in the serum- and membrane-based diagnosis of PDAC. *Cancer Res*; 73(6): 1934–45. ©2012 AACR.

Introduction

Pancreatic adenocarcinoma is one of the few cancers for which the survival rate has not improved in the last 40 years. Around 90% of these pancreatic tumors are pancreatic ductal adenocarcinomas (PDAC; ref 1). While complete surgical removal is the only curative option for this disease, only 15% to 20% of these tumors are resectable at the time of diagnosis (2). The lack of early diagnostic markers poses a major problem for timely detection (3, 4). Therefore, there is an urgent need for the development of novel pancreatic cancer biomarkers that can facilitate early diagnosis and aid in the development of effective therapeutics.

Cancer cell-specific membrane proteins are considered to be the most appropriate biomarkers because they are often shed in body fluids in detectable amounts. By applying mass

spectrometry-based proteomic approaches to pancreatic cancer tissue, serum, juice, urine, and cell lines (5–7), a list of differentially expressed proteins has been identified for PDAC. However, the large datasets obtained using these methods require time consuming verification and validation that generally result in a high rate of false positives and low odds of clinical translation (8). In addition, due to their amphipathic nature (9) and low abundance, membrane proteins have always been under-represented in such comprehensive proteome analysis studies. As an alternative method, specific probes can be developed for membrane proteins that can be used as tools to separate and enrich the bound target protein, which can then be analyzed using conventional techniques.

Nucleic acid probes, aptamers, can bind to its target molecule with high affinity and specificity. Using an *in vitro* iterative selection process known as systematic evolution of ligands by exponential enrichment (SELEX; refs.10–12), aptamers have been generated for a number of disease-associated proteins. In addition to rationally chosen purified proteins, aptamers can also be generated against complex targets such as live cells and tissues using cell-SELEX (13). By applying Cell-SELEX approach to cancer cell lines and cell secretions, novel biomarkers have been identified that can be directly applied to clinical diagnosis and therapeutics (14–17)

Cancer cells are highly heterogeneous in nature and pancreatic cancer cell lines that are in use also show similar variations in genetic and proteomic make-up. Thus, to avoid these variations and to select aptamers that could be targeted to pancreatic adenocarcinoma of ubiquitous presence, we selected aptamers for 2 pancreatic cancer cell lines, Panc-1 and

Authors' Affiliations: ¹Department of Medical Biotechnology, Dongguk University; ²Department of Pathology, Asan Medical Center, University of Ulsan College of Medicine, Seoul; ³Global Research Laboratory of RNAi Medicine, Department of Chemistry, Sungkyunkwan University, Suwon, Korea; and ⁴Department of Medical Biophysics, Ontario Cancer Institute, University of Toronto, Toronto, Canada

Note: Supplementary data for this article are available at Cancer Research Online (<http://cancerres.aacrjournals.org/>).

Corresponding Authors: Dong-ki Lee, Sungkyunkwan University, Suwon 440-746, Korea (South). Phone: 82-31-299-4565; Fax: 82-31-299-4890; E-mail: dklee@skku.edu and Soyoun Kim, Dongguk University, Seoul 100-715, Korea (South). Phone: 82-2-2260-3840; Fax: 82-2-2290-1378; E-mail: skim@dongguk.edu

doi: 10.1158/0008-5472.CAN-12-3682

©2012 American Association for Cancer Research.

Capan-1, in one selection scheme. For counter selection, we used normal human pancreatic ductal cells, HPDE-E6E7-c7 (HPDE; refs. 18, 19). Using this Cell-SELEX approach with a positive/negative selection strategy, we identified a 2'-F-modified RNA aptamer that specifically binds to pancreatic adenocarcinoma cells. An oncofetal antigen, alkaline phosphatase placental-like 2 (ALPPL-2), was identified as the aptamer target protein. ALPPL-2 was found to be a novel PDAC-associated protein whose expression correlates with increased cell growth and invasion. The fact that ALPPL-2 is ectopically expressed on the cell surface of many pancreatic cancer cell lines and can also be detected in cell secretions, makes this oncofetal protein an attractive target for the serum- and membrane-based diagnosis of PDAC.

Materials and Methods

Cell culture

Pancreatic cancer cells obtained from the American Tissue Culture Collection were cultured in humidified conditions at 37°C in a 5% CO₂ atmosphere as indicated: Panc-1 (Dulbecco's Modified Eagle's Medium; DMEM), Capan1 (Iscove's Modified Dulbecco's Medium; IMDM), MiaPaCa-2 (DMEM), Bxpc-3 (RPMI), AsPC-1 (RPMI), Cfpac-1 (IMDM), and Hpaf-II (minimum essential medium) supplemented with 10% or 20% (Capan-1) FBS (Invitrogen) and 100 U/mL penicillin-streptomycin (Invitrogen). HPDE-E6E7-c6 was cultured in keratinocyte serum-free media with growth supplements as described earlier (19).

Cell-SELEX

The starting 2'-F modified RNA library was prepared by *in vitro* transcription of a DNA library containing a 40 nt random region and primer binding sites [5'-ATACCAGCT-TATTCAATT (N₄₀)AG ATAGTAAGTGCAATCT-3'] using Durascribe T7 transcription kit (Epicentre Biotechnologies). A total of 2,000 pmols of this RNA library composed of 10¹⁴ molecules were used for Cell-SELEX (Fig. 1) as described earlier (20). Positive selection was carried out with 2 human pancreatic adenocarcinoma cell lines, Panc-1 and Capan-1, altering each other through the selection rounds. Briefly, the 2'-F RNA library was denatured in binding buffer [4.5 g/L glucose, 5 mmol/L MgCl₂, 0.1 mg/mL yeast tRNA, and 1 mg/mL bovine serum albumin (BSA) in Dulbecco's PBS] at 95°C for 5 minutes. A total of 5 × 10⁶ cells grown as a monolayer were incubated with 500 nmol/L of the library at 4°C for 30 minutes. The unbound sequences were partitioned by 2 successive washes in wash buffer (Dulbecco's PBS containing 4.5 g/L glucose and 5 mmol/L MgCl₂) for 5 minutes each. The cells were then collected by scraping in wash buffer, and the bound RNAs were eluted by heating at 95°C for 5 minutes and separated by phenol:chloroform:isoamyl (PCI) alcohol (Ambion) extraction. The PCI-extracted RNA pool was reverse-transcribed using ImProm-II Reverse Transcription System (Promega) and 5 pmols of N40 reverse primer (5'-AGATTG-CACTTACTATCT-3') and PCR amplified using N40 reverse and forward primer [containing T7 promoter (underlined)

(5'GGTAATACGACTCACTATAGGGGATACCAGCTTATT-CAATT-3')] pairs. The purified PCR product was transcribed *in vitro* and used for the next round. After 10 rounds of continuous positive selection, 2 intermediate negative selections were carried out with 1 × 10⁷ HPDE cells, and the unbound sequences were used for further positive selections until the 14th round. Enrichment in the binders was quantified by quantitative real-time PCR (qRT-PCR). In the 14th round, sequence pool was cloned using a TA Cloning Vector Kit (RBC Bioscience Corp.). Seventy clones were sequenced and analyzed for consensus using Multi-align software (21).

Aptamer K_d determination and size minimization

The screening of potential aptamers and calculation of their binding affinity was done by qRT-PCR. SQ-2 size truncation was done based on its secondary structure predicted by RNA draw V1.1b2 (22). The binding affinity for SQ-2(6-30) was determined by NC-3000 nucleocytometer (ChemoMetec). Detailed protocols are given in Supplementary Methods.

Enrichment of Panc-1(SQ-2-ve), Panc-1(SQ-2+ve) populations of Panc-1

The SQ-2-binding Panc-1 cell population was separated from the nonbinding cells by labeling them with SQ-2-biotin followed by magnetic separation as described in Supplementary Materials and Methods. Panc-1(SQ-2 positive) cells were enriched for 10 such selection rounds to get nearly 100% SQ-2 positive cells. Panc-1(SQ-2 negative) cells were enriched for 3 cycles to reach 100% SQ-2 negative cells. For brevity, these enriched subpopulations are termed as Panc-1 positive and Panc-1 negative.

SQ-2 target pulldown and peptide analysis

Capan-1 cells (~1 × 10⁸ cells) were washed twice with chilled hypotonic buffer [50 mmol/L Tris-HCl (pH 7.5)] and then incubated with the same hypotonic buffer containing protease inhibitors at 4°C for 30 minutes. The buffer was completely removed, and after 2 washes, the cells were lysed in 5 mL of membrane lysis buffer (PBS containing 5 mmol/L MgCl₂ and 1% Triton X-100) containing protease inhibitors at 4°C for 30 minutes. The lysate was clarified by centrifugation and the supernatant was concentrated using 10 kDa centrifugal cut-off filters (Amicon). The concentrated membrane lysate was incubated with 200 pmols of SQ-2(6-35)-biotin or biotinylated mutant oligo (St Pharm Inc.) at 4°C for 30 minutes along with a 100-fold excess concentration of yeast tRNA (Invitrogen). The SQ-2-protein complex was captured by further incubating with 25 μL of preblocked streptavidin-agarose beads (Thermoscientific) at 4°C for 60 minutes. The SQ-2-protein-agarose bead complex was collected by centrifugation and washed 4 times with the lysis buffer. The SQ-2(6-35) or mutant oligo-bound proteins were eluted from the complex by incubation with 50 units of RNase I (MBI-Fermentas) at 37°C for 10 minutes. The eluate was partitioned from the beads by centrifugation and analyzed on 4% to 15% SDS-PAGE. Peptide analysis of the SQ-2 pull-down protein was done by liquid chromatography-electrospray-tandem mass

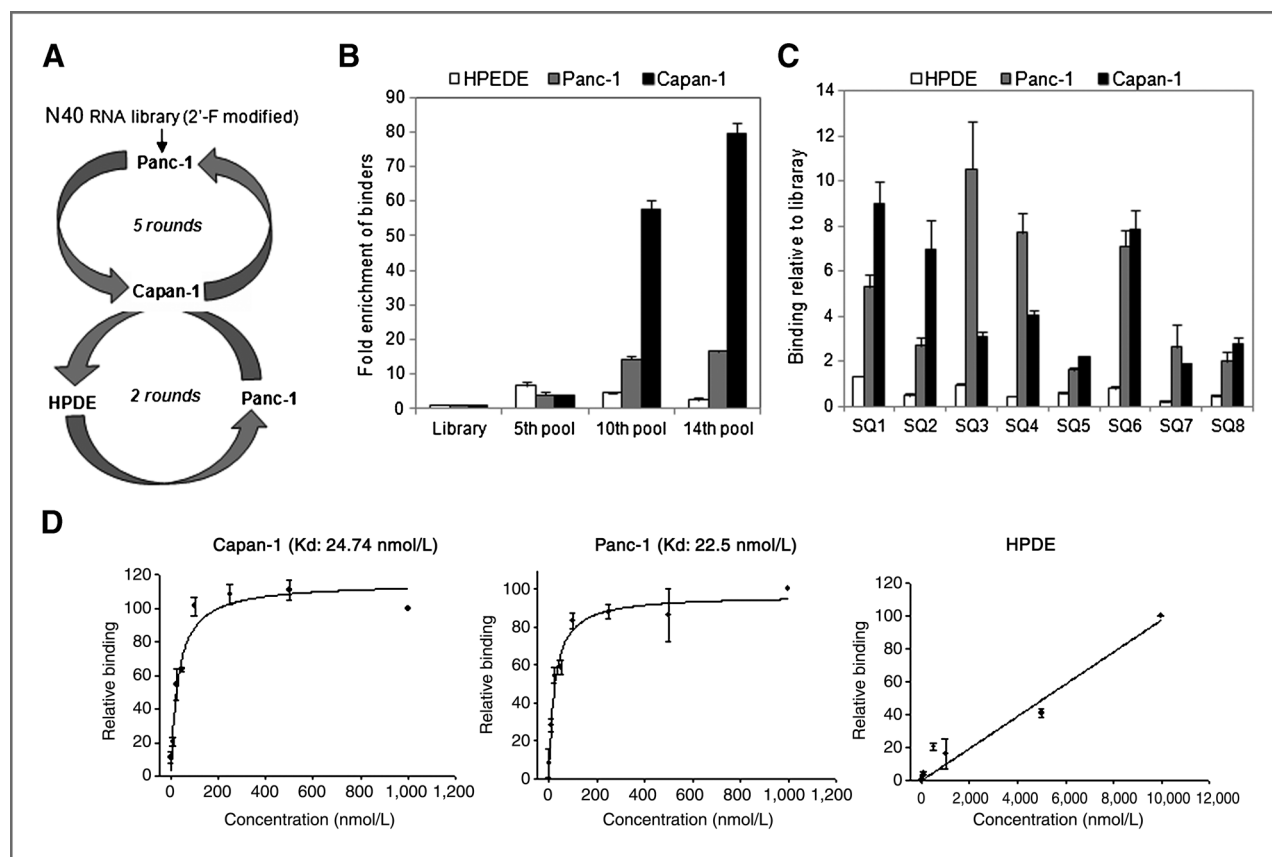


Figure 1. Cell-SELEX based identification of PDAC specific aptamer SQ-2. A, pancreatic cancer cell-SELEX scheme. B, enrichment of binders through SELEX. A total of 50 nmol/L of the starting RNA library and the 5th, 10th, and 14th round pools were tested for binding to Capan1, Panc1, and HPDE by RT-PCR. Binding relative to the starting library is shown. C, binding efficiency and specificity of the 8 selected aptamers for Capan1 and Panc-1 in comparison with HPDE. D, cells were incubated with increasing concentrations of SQ-2 and the binding was analyzed by RT-PCR. The ligand binding curves and K_d values obtained for Panc-1 and Capan1 are shown. No saturation in binding was observed with HPDE until a 10 μ mol/L concentration. Data are represented as mean \pm SE of 3 independent measurements.

spectrometry and a MASCOT database search facility from ProteomeTech Inc.

Genome-wide microarray

For aptamer target identification, total RNA was extracted using TRI Reagent and an RNeasy mini kit (Qiagen, GmbH, Hilden) in accordance with the manufacturer's protocols. Total RNA was processed for double-stranded cDNA synthesis and labeling in accordance with NimbleGen Arrays User's guide, as described earlier (23). Expression data were normalized through quantile normalization and Robust Multichip Average algorithm (24). mRNAs with more than a 2-fold difference in expression in Capan-1, Panc-1, Panc-1-negative, and Panc-1-positive cells relative to HPDE were identified and arranged in order of most to least differential expression in Panc-1-positive relative to Panc-1-negative cells. To identify ALPPL-2-regulated genes via siRNA-based gene knockdown, Panc-1-positive cells were transfected with ALPPL-2 or siGFP control siRNAs for 48 hours, followed by RNA extraction and microarray sample preparation as described above. Genes that showed 1.5-fold or more differential expression with both the ALPPL-2-targeting siRNAs relative to siGFP and transfection reagent controls were visu-

alized with Java tree view and functionally categorized using a web-based program, Database for Annotation, Visualization and Integrated Discovery (25). Enrichment in gene ontology terms, for differentially expressed genes, was seen at Fisher exact $P < 0.05$ and count threshold 2. Gene expression data sets have been deposited in the Gene Expression Omnibus.

siRNA transfection and qRT-PCR

Panc-1-positive cells were transfected with 10 nmol/L of siRNAs using the Lipofectamine 2000 reagent at the concentrations indicated by the manufacturer (Invitrogen). siRNA electroporation was done according to ref. (26) with some modifications. Total RNA was extracted using isol-RNA lysis reagent (ref. 5; PRIME Inc.), reverse transcribed, and analyzed by qRT-PCR. qPCR data for each gene product were normalized with GAPDH mRNA or 18S rRNA. Detailed protocols are given in Supplementary Methods.

Fluorescence microscopy and nucleocounter NC3000 analysis

Cells grown on glass bottom petri dishes were incubated with 50 nmol/L of 3'-TAMRA-labeled SQ-2(6-30) or the mutant

Table 1. Aptamer sequences identified by cloning final SELEX product

Sequence family	Aptamer sequence	Percentage of total sequences	Binding affinity (nmol/L)	
			Panc-1	
			Capan-1	
SQ-1	AUACCAGCUUAUUCAAUUGCCUGAUUAGCCGUAUCACGAUUAACUUAACCUUCGUUGCUGAGAUAGUAAGUGCAAUCU	36.36	72 ± 10	81.5 ± 4.94
SQ-2	AUACCAGCUUAUUCAAUUGCCUGAAAGCUAUCGCCCAUUCGCAGUGAUUAUCUUUAAGAUAGUAAGUGCAAUCU	12.09	22.5 ± 4.5	24.74 ± 2.2
SQ-3	AUACCAGCUUAUUCAAUUGCCUGAAACCCUGUCUCUCUGCAGCAAGACUAUGTUGAGAUAGUAAGUGCAAUCU	9.8	60.64 ± 16.9	29.98 ± 5.4
SQ-4	AUACCAGCUUAUUCAAUUGCCUGAGUAGCUGGGUCCGCCACACAUUACCAUUAUUGAGAUAGUAAGUGCAAUCU	9.8	96.5 ± 15.5	61.5 ± 3.5
SQ-5	AUACCAGCUUAUUCAAUUGCCUGAAACCCUGUCUCUCUUAUUGCCUUAUUCUUAUUCUGGAGAUAGUAAGUGCAAUCU	6.8	49 ± 5.8	21.3 ± 5.07
SQ-6	AUACCAGCUUAUUCAAUUGCCUGAAGACUJGGAUUAACUUAAGCAUUAUUAUUCGAGAUAGUAAGUGCAAUCU	4.54	210.5 ± 32.3	56.5 ± 6.5
SQ-7	AUACCAGCUUAUUCAAUUGCCUGAAACUJGUGAUCGUCUCCACGUAUACACAUUGAAGAUAGUAAGUGCAAUCU	4.54	36.5 ± 4.05	5.87 ± 2.09
SQ-8	AUACCAGCUUAUUCAAUUGCCUGAAAGUUUAACUCCAAAUAACGCCGUGAGAUAGUAAGUGCAAUCU	4.54	87 ± 2.82	46.32 ± 3.9

sequence in culture medium for 20 minutes at 37°C. Following 2 quick washes, images were acquired using fluorescence microscope (Olympus IX-81) and Metaview imaging software at ×200 or ×400 magnification. To quantify the reduction in aptamer binding upon ALPPL-2 knockdown, cells were incubated with 50 nmol/L of TAMRA-labeled SQ-2 (6-30) and 10 μg/mL of Hoechst 33342 for 20 minutes at 37°C. Cells were washed with culture media 2 times and collected by gentle scraping. The cell pellet was resuspended in 100 μL of culture medium and immediately analyzed on Nucleocounter NC-3000 (Chemometec) using user adaptable protocols. Five thousand cells were analyzed and the mean fluorescence intensity of cells with SQ-2-TAMRA binding was calculated.

Invasion assay

Panc-1-positive cells transfected with ALPPL-2 siRNAs for 72 hours were resuspended in DMEM containing 0.1% BSA. A total of 1×10^5 cells were added on to Matrigel-coated polyethylene tetraphthalate filters of 8 μmol/L pore size (BD falcon) in a 24-well plate. Serum containing 10% DMEM was used as a chemoattractant in the lower chamber. After 18 to 20 hours of incubation, the inserts were stained with 0.1% crystal violet solution in methanol. Cells from the underside of the membrane were counted under microscope and are represented as the number of invaded cells.

Results

Aptamer selection and characterization

To select PDAC-specific aptamers, we used 2 pancreatic cancer cell lines, Panc-1 and Capan-1, for positive selections. The SELEX process began with selection for Panc-1-binding 2'-F-modified RNA sequences. The Panc-1-selected RNA pool was used for positive selection for Capan-1. Ten rounds of positive selection (5 with Capan-1 and 5 with Panc-1) were conducted (Fig. 1A). The RNA pool obtained from the 10th positive selection was used for counter selections with HPDE cells, and the unbound RNA pool was directly used for positive selections. Two such alternating negative/positive selection cycles were conducted.

The enrichment of binders during the selection process was measured using qRT-PCR. The starting N40 library and the 5th, 10th, and 14th round pools were tested for binding to Panc-1, Capan-1, and HPDE cells. Both Panc-1 and Capan-1 cells showed an increase in the percentage of binders with increasing cycles when compared with the starting library (Fig. 1B). Because the 14th round pool showed significant enrichment, the SELEX process was discontinued, and the RNA pool was cloned and sequenced. Sequences were aligned into families according to sequence homology. As shown in Table 1, 8 distinct sequences were identified; their binding to Capan-1 and Panc-1 was 2 to 11 times higher than that of the initial library (Fig. 1C). Aptamer binding was also confirmed by fluorescence microscopy using a TAMRA-labeled reverse primer annealed to the aptamer sequences (data not shown). Finally, based on the aptamer specificity for Panc-1 and Capan-1 cells relative to HPDE and the

binding affinity, the SQ-2 aptamer was chosen for further analysis. The saturation curves of SQ-2 for Capan-1 and Panc-1 show a K_d value of 24.7 and 22.5 nmol/L, respectively. Concentration-dependent binding with no saturation even up to a 10 μ mol/L concentration indicates a nonspecific binding for HPDE (Fig. 1D).

SQ-2 structure-based serial truncations identified 25 nt miniaturized aptamer SQ-2(6-30), with binding affinity and specificity similar to the full-length form

The predicted secondary structure of full-length SQ-2 (78 nt) shows folding into a 3-way stem loop structure (Fig. 2A). To further use the aptamer in target identification, imaging, or therapeutics, the full-length SQ-2 needed to be reduced to a size amenable for chemical synthesis with minimal loss in target binding. Several serially truncated versions of the SQ-2 aptamer were generated and tested for binding to Capan-1. Deletions of the primer-binding regions indicated that the

aptamer random region alone is insufficient to bind to the target cell. Although the 3'-primer-binding region was dispensable, deletion of the 5'-primer-binding region completely abolished aptamer binding (Fig. 2B), suggesting that the 5'-primer-binding region may be a part of the aptamer target-binding domain. Additional structures based on stem-loop truncations from the 3'-end or 5'-overhang revealed a 25 nt minimal binding domain SQ-2(6-30), which showed binding similar to full-length SQ-2 (Fig. 2B and C). The binding affinity of the chemically synthesized minimized aptamer SQ-2(6-30) was determined to be 20 nmol/L for Capan-1 cells, which is similar to that of full length SQ-2 (Fig. 2D). Fluorescence microscopic analysis of SQ-2(6-30) binding to Capan-1 and Panc-1 showed distinct binding to the cell membrane (Fig. 2E). Interestingly, although the aptamer bound to 100% of the Capan-1 cell population, it only recognized a subset of Panc-1 cells. No binding was seen with HPDE cells.

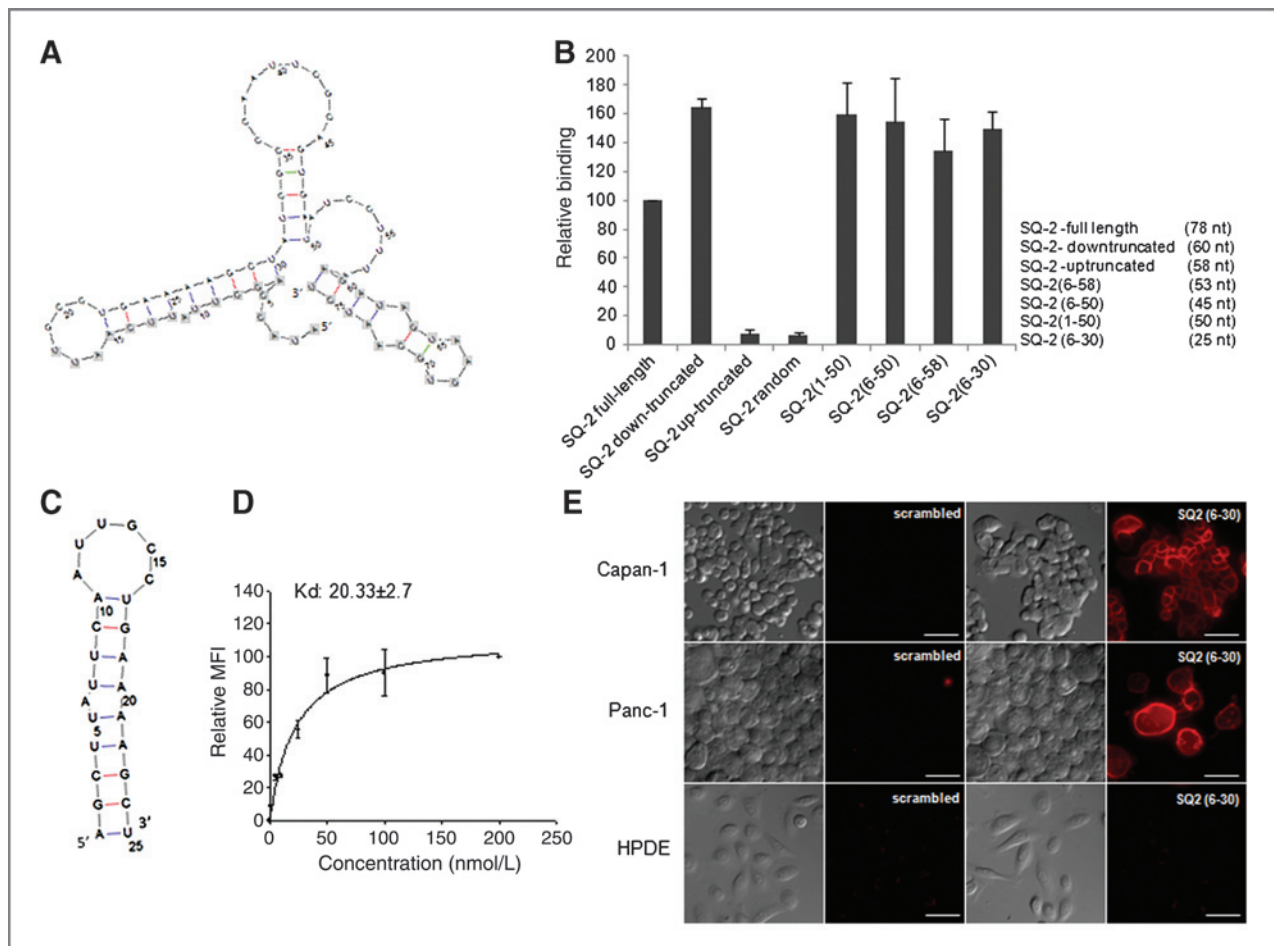


Figure 2. SQ-2 structure-based size minimization to SQ-2(6-30). A, two-dimensional structure of full-length SQ-2 as predicted by RNA draw. The 5' and 3' primer-binding regions are marked in gray boxes. B, SQ-2 devoid of primer binding regions or 3' end stem loops were tested for binding to Capan-1 relative to full-length SQ-2 by RT-PCR. The final length of truncated versions is indicated. C, two-dimensional radial drawing of the 25 nt long final truncated structure SQ-2(6-30). D, binding affinity of chemically synthesized SQ-2(6-30)-TAMRA was calculated by nucleocyctometer. E, fluorescence microscopic analysis of SQ-2(6-30) binding. Cells grown on glass bottom petri dishes were incubated with 50 nmol/l of SQ-2(6-30)-TAMRA. A scrambled SQ-2 sequence was used as nonspecific binding control. Images were acquired at $\times 400$ magnification and the scale bar represents 50 μ mol/L.

Table 2. Mass-spectroscopy analysis data of SQ-2 specific bands B1 and B2

	Protein	MWt	Matches	Score
B1 MS data				
gi 119591402	Alkaline phosphatase, placental-like 2, isoform CRAc	57212	38	329
gi 13786807	Chain A, Crystal structure of a human phosphatase	55556	38	312
gi 6453491	Hypothetical protein	31469	2	26
gi 2114239	POM121-like 2	22011	1	24
B2 MS data				
gi 11935049	Keratin-1	66027	9	168
gi 119591402	Alkaline phosphatase, placental-like 2, isoform CRAc	57212	3	72
gi 28317	Unnamed protein product	59492	3	59
gi 22028256	Similar to heterogeneous nuclear ribonucleoprotein U	58286	3	50
gi 18916718	KIAA1939 protein	122909	2	34
gi 12803709	Keratin-14	51619	2	34

SQ-2 target identification via aptamer-mediated membrane protein pull-down and analysis of differentially expressed mRNA in Panc-1-negative and -positive cells

The complete loss in SQ-2(6-30) binding to protease K-treated Capan-1 cells confirmed that the target is a membrane protein (Supplementary Fig. S1). In addition, only partial loss in binding to trypsin-treated cells indicates that either the target protein has some resistance toward trypsin or is present in membrane domains that are inaccessible to trypsin. Further identification of the target protein was conducted via SQ-2(6-35)-biotin and streptavidin-agarose-based pull-down from the membrane lysate. A nonfunctional mutant SQ-2(6-35) served as a control for nonspecific oligonucleotide-binding proteins. Aptamer-bound proteins were eluted by RNase I treatment and finally resolved on a precast gradient gel under denaturing conditions. Colloidal Coomassie staining revealed a distinct band around 65 kDa that was present in the SQ-2 pull-down but not in the mutant (marked as B1, Fig. 3A). In addition, the absence of this band in the presence of high concentrations of biotin-free SQ-2 competitor confirms that this is the target protein. We also identified a faint band at 130 kDa that was specific to SQ-2 (marked as B2). Mass spectroscopic analysis of these bands, B1 and B2, revealed a common match of ALPPL-2 (Table 2).

ALPPL-2 is known to be present on cell membranes via glycosylphosphatidylinositol (GPI) anchors in monomeric and dimeric forms. They undergo dimerization by hydrogen bonding and Van der Waals linkages (27) and are structurally very heat resistant (28). Furthermore, ALPPL-2 that contains 2 asparagine-linked glycosylation, migrates on gel as a 65 kDa product (29). The membrane localization of ALPPL-2, its occurrence as a dimer, the correlation between its actual size (57 kDa) and that of the glycosylated protein on gels (65 kDa, 130 kDa), and its resistance to heat and mercaptoethanol all suggest that both the bands B1 and B2 are ALPPL-2.

In a parallel strategy, we tried to identify the target by taking advantage of Panc-1 heterogeneity. Only a subpopulation of Panc-1 cells show binding to SQ-2, suggesting that the target protein expression is limited to a certain clonal population in this cell line. On the basis of this clonal difference, SQ-2-positive and SQ-2-negative Panc-1 cell line clones were separated by live cell pull-down. Repeated selections resulted in pure Panc-1-positive and Panc-1-negative cell lines (Fig. 3B). Using genome-wide microarray, we compared the mRNA expression in these Panc-1 sublines and in Capan-1 and HPDE. Genes with 2-fold or more differential expression in Panc-1-positive relative to Panc-1-negative cells resulted in 450 transcripts. The top 10 differentially expressed transcripts in Panc-1-positive cells are listed in Supplementary Table S1. ALPPL-2 was the second and third transcript on the list with more than a 500-fold difference in expression. Although placental alkaline phosphatase (ALPP), another member of ALPP family, was first on the list, 2 of the 3 ALPP probes used in the chip had a 100% match to ALPPL-2.

Target validation by ALPPL-2 gene knockdown and immunoassay

The SQ-2-bound target protein was confirmed to be ALPPL-2 by aptamer-based pull-down, followed by Western blot analysis with ALPPL-2 antibody. The ALPPL-2 band was observed in SQ-2 pull-downs of Capan-1 and Panc-1-positive cells but not in Panc-1-negative cells (Fig. 4A). Furthermore, we designed siRNAs that could specifically silence ALPPL-2 in Panc-1-positive cells, and tested SQ-2 binding in ALPPL-2 knockdown conditions. More than 80% knockdown in ALPPL-2 mRNA and protein was seen with siALPPL-2-2 and siALPPL-2-3 (Fig. 4B and C). Fluorescence microscopy and nucleocytochrome analysis of Panc-1-positive cells transfected with these siRNA showed 90% loss in aptamer binding (Fig. 4D and E), confirming that SQ-2 binds to ALPPL-2.

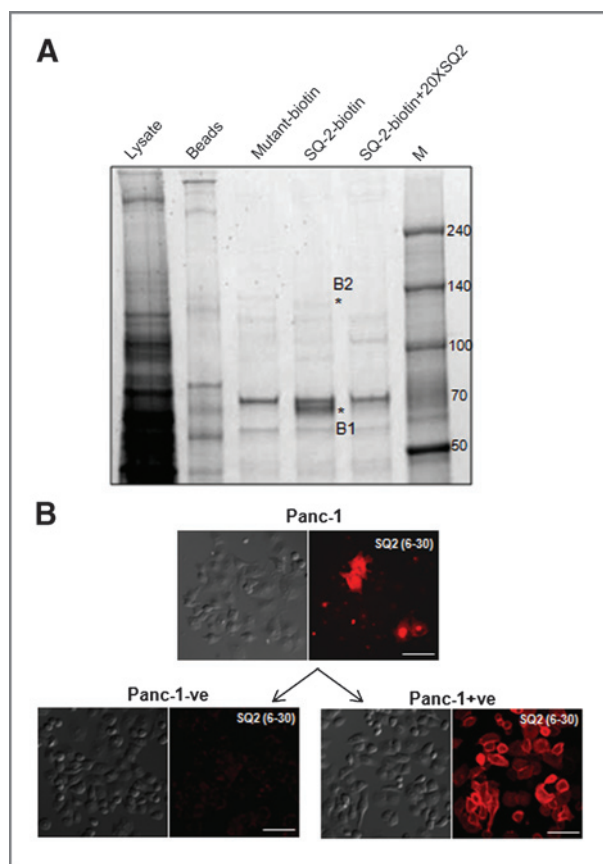


Figure 3. Aptamer SQ-2 target identification from Capan-1 and Panc-1+ve cells. **A**, Capan-1 membrane lysate was incubated with SQ-2(6-35)-biotin for 30 minutes at 4°C. The bound protein was pulled-down using streptavidin agarose beads and resolved on denaturing gradient SDS-PAGE. Colloidal Coomassie blue staining of gel identified SQ-2-specific bands B1 and B2, marked as asterisk at 65 kDa and 130 kDa, respectively. A nonfunctional SQ-2 mutant was used as control for nonspecific oligonucleotide-binding proteins. Incubation with a 20-fold higher concentration of free SQ-2 inhibits the SQ-2-biotin mediated pull-down of B1 and B2. Results are representative of 3 independent pull-down experiments. **B**, enrichment of Panc-1 to Panc-1 positive and Panc-1 negative populations by SQ-2-biotin-mediated live cell pull-down and magnetic separation. SQ-2 Positive and SQ-negative cell lines were obtained after 10 and 3 enrichment rounds, respectively. SQ-2-TAMRA binding confirms the purity of the Panc-1 subpopulations. Scale bar represents 100 $\mu\text{m/L}$.

SQ-2 binds to both ALPPL-2 and ALPP

ALPP and ALPPL-2 proteins differ by only 10 amino acids resulting in 98% homology (27). Because of this high structural similarity, immunoassays fail to specifically identify one isozyme in the presence of the other (30, 31). They can only be clearly differentiated by using gene-specific primers (31). To determine the specificity of SQ-2 for these isozymes, we first checked the mRNA expression of ALPP and ALPPL-2 by using specific primer sets. qPCR was carried out using these primers; the C_t values show that while only ALPP is expressed in HPDE, both of the isozymes are expressed in Capan-1 and Panc-1 (Supplementary Fig. 2A). Moreover, the SQ-2-based selection of Panc-1-positive and Panc-1-negative cell types led to a significant difference in expression of ALPPL-2 in these sub-

lines, but only a marginal difference in the case of ALPP (Supplementary Fig. 2B). This suggests that either the aptamer has poor affinity for ALPP or the selection was driven by ALPPL-2 due to its higher basal expression over ALPP.

Next, we screened some ALPP-targeting siRNAs in Panc-1-positive cells and found one siRNA that could specifically knockdown ALPP mRNA levels by 80% without affecting ALPPL-2 mRNA (Supplementary Fig. S2C). ALPP knockdown in Panc-1-positive cells did not affect the binding of SQ-2-TAMRA. In addition, the transfection of ALPP and ALPPL-2 siRNAs together did not further reduce SQ-2 binding in comparison with that of siALPPL-2 alone (Supplementary Fig. S2D). We suspected that more than a 3-log increase in the expression of ALPPL-2 may have masked the effect of ALPP knockdown on SQ-2 binding. Therefore, we conducted the same study in Capan-1, where ALPP and ALPPL-2 have similar expression levels. However, because this cell line is hard to transfect using standard transfection reagents, we conducted siRNA electroporation and obtained 70% and 60% silencing of ALPPL-2 and ALPP, respectively (Supplementary Fig. S2E). An SQ-2-TAMRA-binding study under both ALPP and ALPPL-2 knockdown conditions showed significant reductions in SQ-2 binding (Supplementary Fig. S2F). The knockdown of both the isozymes together showed nearly complete loss in binding, confirming that both ALPPL-2 and ALPP bind to SQ-2. However, the identification of only ALPPL-2 in the mass spectrometric analysis of SQ-2 pull-downs from Capan-1 cells and the preferential enrichment of ALPPL-2 in Panc-1-positive cells suggests that SQ-2 may have a higher affinity for ALPPL-2.

ALPPL-2 is ectopically expressed in PDAC cells and can also be detected in the cell secretome

ALPPL-2 mRNA and protein expression was checked in other PDAC cell lines. In addition to Capan-1 and Panc-1, 3 more PDAC cell lines, HPAF-II, BxPC-3, and AsPC-1, showed ectopic expression of ALPPL-2 mRNA and protein (Fig. 5A and B). Fluorescence microscopic analysis of SQ-2 binding to these cells showed a heterogenic pattern similar to Panc-1 with around 10% to 20% SQ-2-positive population across these cells (Supplementary Fig. S3). However, no significant ALPPL-2 mRNA or protein could be detected in MiaPaCa2 and CFPAC-1 cells. The monoclonal ALPPL-2 antibody used in our study recognizes a stretch of 365 to 455 amino acids, which is similar to that of ALPP except at position 429 where glycine is replaced with glutamine. Studies have shown that although this single amino acid difference imparts some degree of specificity to the ALPP and ALPPL-2 antibodies, they can still bind to the other isozyme with a slightly reduced affinity (32). Therefore, the protein levels of ALPPL-2 studied using this antibody may have been affected by the presence of ALPP. As none of the currently available antibodies can clearly differentiate between these isozymes, it is hard to validate the results of these immunoassays (30, 31).

Placental ALPPs are known to be secreted and has shown a potential use for serum-based diagnosis of seminomas (33). Therefore, we also checked whether ALPPL-2 could be detected from the cell secretions of PDAC cells. Conditioned medium prepared from both Capan-1 and Panc-1-positive

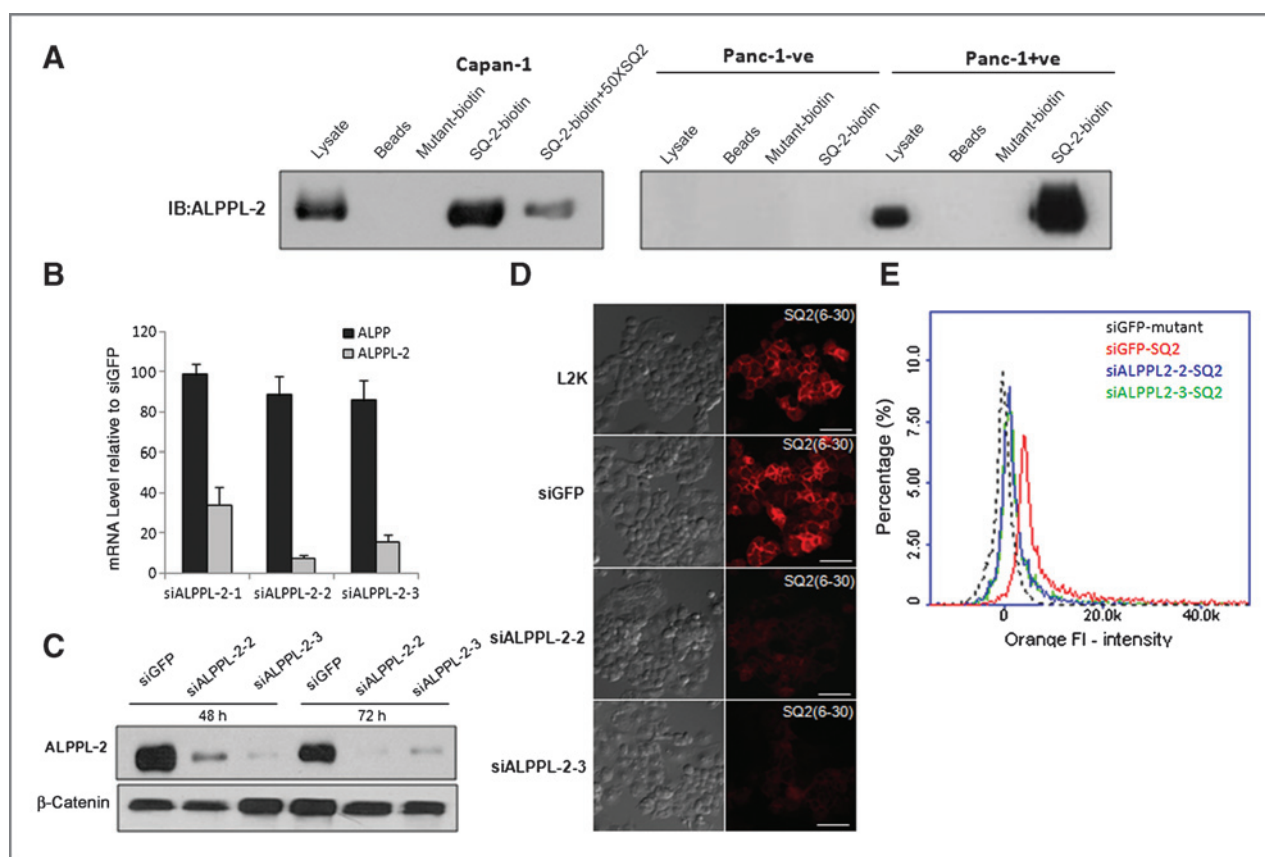


Figure 4. ALPPL-2 antibody and siRNA-based validation of the target. **A**, immunoassay of SQ-2-biotin-mediated protein pull-down from membrane lysate confirms the target protein as ALPPL-2. **B**, siRNAs were designed to specifically silence ALPPL-2 but not ALPP and their target silencing efficiency was measured by RT-PCR at 10 nmol/L concentrations. siGFP was used as a nonspecific siRNA control. ALPP and ALPPL-2 mRNA levels relative to siGFP transfection are shown as mean \pm SD of 3 independent experiments. **C**, Panc-1 positive cells transfected with siALPPL-2-2 and siALPPL-2-3 for 72 hours were checked for ALPPL-2 protein knockdown by Western blot analysis. **D**, Panc-1 positive cells transfected with ALPPL-2 and siGFP control for 72 hours were incubated with 50 nmol/L of SQ-2 (6-30)-TAMRA. Images were acquired using fluorescence microscope at $\times 200$ magnification. The scale bar represents 100 μ m/L. **E**, SQ-2-TAMRA binding was quantitated using nucleocytometer.

cells showed that ALPPL-2 was present in easily detectable amounts (Fig. 5C). Furthermore, SQ-2-mediated ALPPL-2 pull-down from the cell secretions indicates that both the aptamer and the antibody can be used for the detection of ALPPL-2 in the PDAC secretome.

ALPPL-2 regulates cell growth and invasion in PDAC cells

Although ALPPL-2 was found to be present in certain tumor tissues and cell lines, the physiologic significance of their expression and release remains obscure. To understand the role of ALPPL-2 in PDAC progression, we studied cell growth in Panc-1-positive cells transfected with ALPPL-2 siRNAs. A Trypan blue dye exclusion assay of cells 72 hours posttransfection showed about a 20% reduction in cell number in ALPPL-2 knockdown conditions (Fig. 6A). Panc-1-negative cells that lack ALPPL-2 expression also showed increased necrosis and cell senescence with due passages (data not shown), suggesting that ALPPL-2 has some association with cell growth and maintenance in PDAC cells. We also studied the invasive potential of ALPPL-2 knockdown cells and found about a

50% reduction in Matrigel invasion in comparison with cells transfected with control siRNA (Fig. 6B). However, treatment of Panc-1-positive cells with SQ-2 had no effect on cell viability or invasion (data not shown), suggesting that the aptamer itself is not inhibitory to ALPPL-2 function.

Genome-wide microarray analysis of differentially expressed mRNA in Panc-1-positive cells transfected with siALPPL-2 or control siRNAs resulted in a list of genes with a 1.5-fold or more reduction in mRNA levels (Fig. 6C). Functional categorization of these differentially expressed genes identified the enrichment of gene ontology terms like cytokine, peptide binding, and JAK-STAT activity (Supplementary Table S2). We picked some key downregulated genes and validated them using qRT-PCR. Figure 6D shows that the expression of interleukin 1 and 6 receptors that mediate cytokine signaling (34, 35), and activation of Janus kinase (36), were reduced upon siALPPL-2 transfection. In addition, mRNA expression of genes involved in cell-cycle progression, namely S-phase kinase-associated protein 2 (SKP2), cyclin D2 (CCND2; refs. 37, 38), were also affected upon ALPPL-2 knockdown. A reduction in the mRNA levels of antiapoptotic

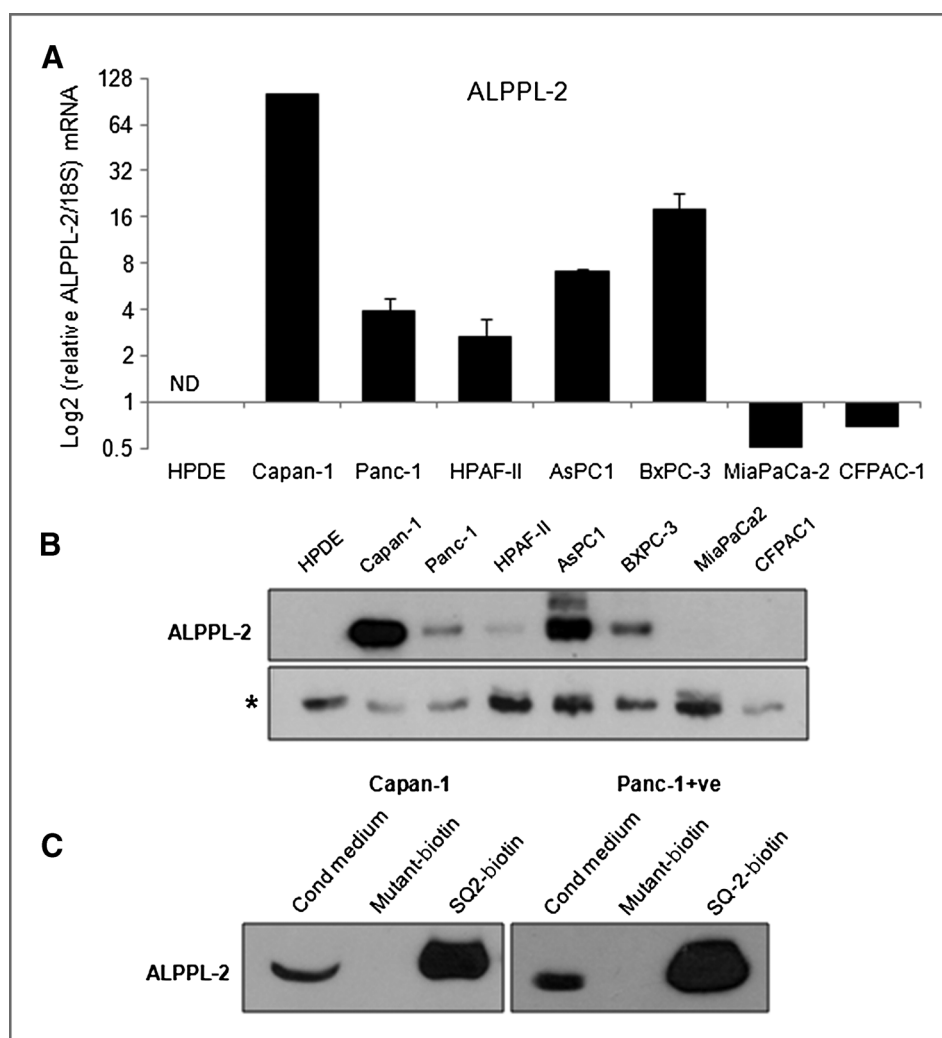


Figure 5. ALPPL-2 is ectopically expressed in pancreatic cancer cells and can also be detected in the cell secretome. **A**, ALPPL-2 mRNAs in pancreatic cancer cell lines were measured using qRT-PCR. The mRNA levels relative to Capan-1 are shown as the mean \pm SD of 3 independent experiments. No ALPPL-2 mRNA was detected in HPDE cells (ND). **B**, ALPPL-2 Western blot analysis of membrane lysate of pancreatic cell lines. A low molecular weight nonspecific band (*) was used as equal loading marker. **C**, conditioned media obtained from Capan-1 and Panc-1 positive cells was concentrated and subjected to SQ-2(6-35)-biotin-mediated target protein-down. Western blot analysis of the conditioned media and the pull-downs confirm the presence of ALPPL-2 in the secretome.

protein BCL-2-related protein A1(BCL2A1; ref. 39) was also observed.

Discussion

The misregulation of embryonic genes plays a significant role in the cancer process (40, 41). As these oncofetal antigens are eutopically or ectopically expressed, they serve as very useful biomarkers in cancer diagnosis. Members of the ALPP class have also been recognized as oncofetal antigens. Placental (ALPP) and placental like (ALPPL-2) alkaline phosphatases seem to be associated with the malignancy of germ cells and some nongerm cell tissues. ALPPL-2 has been found to be overexpressed in testicular cancers and seminoma of the testis (42, 43). Ovarian cancers often show coexpression of ALPP and ALPPL-2 (44). These ALPPs are GPI-anchored membrane proteins that can dimerize and are secretory in nature (45). Using aptamer-based biomarker identification, we found that ALPPL-2 is also expressed in PDAC. Interestingly, ALPPL-2 expression in PDAC was found to be of ectopic nature as no mRNA or protein expression could be detected in nonneoplastic HPDE cells. An earlier report on a panel of PDAC cell lines

and tissue samples analyzed by serial analysis of gene expression also identified ALPPL-2 as the most differentially expressed gene (46). This corroborates our finding and highlights the clinical relevance of ALPPL-2 as a biomarker. More importantly, identification of these ALPPs in precancerous conditions of the colon (47) and in carcinoma *in situ* of the testis, a condition that precedes all cases of testicular tumors (43, 47), suggests its probable use in the early detection of PDAC.

Although the ectopic occurrence of ALPPL-2 in PDAC is intriguing, similar occurrences of ALPP in breast cancer and bronchogenic carcinomas have been reported earlier and have been interpreted as a consequence of the derepression of the tumor cell genome (47). To date, there is no clear information about the molecular switch that regulates ALPPL-2 expression in these nongerm cell tissues. Moreover, the association of ALPPL-2 with malignancy has never been explored. Therefore, we tried to understand the role of ALPPL-2 in PDAC and found that ALPPL-2 promotes pancreatic cancer cell growth and invasion. Human trophoblastic cells overexpressing ALPP show similar effects on cell growth and proliferation (48).

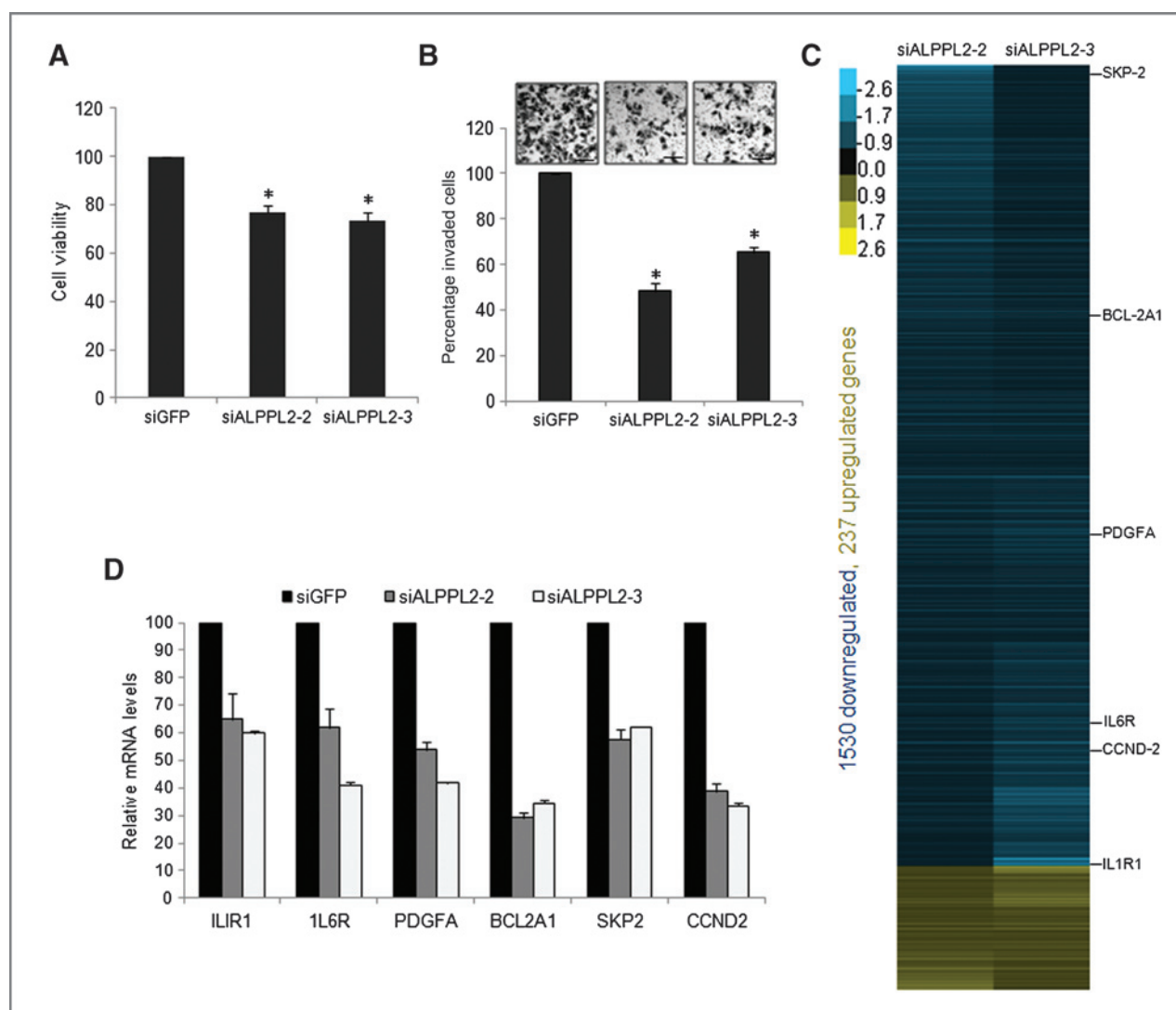


Figure 6. ALPPL-2 regulates the proliferation and invasion of PDAC cells. A, Panc-1 positive cells transfected with ALPPL-2 siRNA for 72 hours were counted by Trypan blue dye exclusion assay. Viable cells relative siGFP control are shown as the average of 3 independent experiments. *, $P < 0.005$ (paired t test) vs. siGFP control. B, Panc-1-positive cells transfected with ALPPL-2 siRNAs were checked for invasion through Matrigel-coated culture inserts. The number of invaded cells and a phase contrast image of a representative field at $\times 10$ magnification. The scale bar represents $200 \mu\text{mol/L}$. *, $P < 0.015$ (paired t test), relative to siGFP control. C, mRNA levels in Panc-1-positive cells transfected with ALPPL-2 siRNAs were analyzed by microarray. Transcripts with more than a 1.5-fold changes in expression in both the siRNAs relative to the siGFP control were collected and are shown in a tree view. D, validation of some key genes was done by RT-PCR and their mRNA levels relative to the siGFP-transfected control are shown as the average of 3 independent experiments.

Genome-wide microarray-mediated analysis of ALPPL-2 function revealed that genes related to cytokine signaling and cell-cycle progression were associated with ALPPL-2 expression. Although ALPPL-2 has been known as an oncofetal antigen since the 1980s, this is the first report that shows the tumor-associated functions of this protein. Detailed analysis of ALPPL-2-mediated regulation of these molecules and associated signaling pathways will further develop our understanding of the presence and role of this protein in tumorigenesis. The nonuniform expression of ALPPL-2 in PDAC cell lines is also of interest and can be mostly attributed to the heterogeneous nature of PDAC (49). However, as ALPP is a marker for embryonic and cancer stem cells (50), the possibility that these

ALPPL-2 expressing cells may serve as cancer stem cells cannot be ignored.

Unlike traditional proteomic approaches, aptamer-based biomarker identification relies on the molecular recognition of the target from a complex proteome, which allows for the identification of both quantitative and qualitative differences between normal and diseased proteomes. Counter selection with the normal proteome in cell-SELEX facilitates the identification of less abundant biomarkers that are generally missed by most mass-spectrometric techniques due to the "masking effect" created by more abundant proteins. This could be the reason as to why ALPPL-2 has not been earlier identified as a PDAC-associated protein by standard proteomic

approaches. Even though it is not an abundant protein and has highly heterogeneous expression in Panc-1 cells, its ectopic expression in PDAC cells favored the selection of ALPPL-2-binding aptamers in the SELEX process. The aptamer SQ-2, identified by our cell-SELEX approach, has good affinity for ALPPL-2 and can recognize the target in both its membrane-bound and secretory forms. Therefore, besides having potential use as a diagnostic tool, it also has straightforward applications in imaging and therapeutics. Moreover, the use of SQ-2 aptamer is not limited to PDAC alone as it can be used for all other cancers that have aberrant expression of ALPPL-2. While RNAi-mediated protein knockdown studies suggest that SQ-2 also binds to ALPP, overall it seems that there could be some differences in its binding affinity for the 2 isozymes. Further investigation in this area will provide a clear understanding of its isozyme-specific bias, if any.

Disclosure of Potential Conflicts of Interest

No potential conflicts of interest were disclosed.

References

- Bardeesy N, DePinho RA. Pancreatic cancer biology and genetics. *Nat Rev Cancer* 2002;2:897-909.
- Li D, Xie K, Wolff R, Abbruzzese JL. Pancreatic cancer. *Lancet* 2004;363:1049-57.
- Brand R, Mahr C. Risk factors for pancreatic adenocarcinoma: are we ready for screening and surveillance? *Curr Gastroenterol Rep* 2005;7:122-7.
- Lee MX, Saif MW. Screening for early pancreatic ductal adenocarcinoma: an urgent call! *JOP* 2009;10:104-8.
- Gronborg M, Bunkenborg J, Kristiansen TZ, Jensen ON, Yeo CJ, Hruban RH, et al. Comprehensive proteomic analysis of human pancreatic juice. *J Proteome Res* 2004;3:1042-55.
- Gronborg M, Kristiansen TZ, Iwahori A, Chang R, Reddy R, Sato N, et al. Biomarker discovery from pancreatic cancer secretome using a differential proteomic approach. *Mol Cell Proteomics* 2006;5:157-71.
- Weeks ME, Hariharan D, Petronijevic L, Radon TP, Whiteman HJ, Kocher HM, et al. Analysis of the urine proteome in patients with pancreatic ductal adenocarcinoma. *Proteomics Clin Appl* 2008;2:1047-57.
- Whiteaker JR, Lin C, Kennedy J, Hou L, Trute M, Sokal I, et al. A targeted proteomics-based pipeline for verification of biomarkers in plasma. *Nat Biotechnol* 2011;29:625-34.
- le Coutre J, Whitelegge JP, Gross A, Turk E, Wright EM, Kaback HR, et al. Proteomics on full-length membrane proteins using mass spectrometry. *Biochemistry* 2000;39:4237-42.
- Ellington AD, Szostak JW. *In vitro* selection of RNA molecules that bind specific ligands. *Nature* 1990;346:818-22.
- Tuerk C, Gold L. Systematic evolution of ligands by exponential enrichment: RNA ligands to bacteriophage T4 DNA polymerase. *Science* 1990;249:505-10.
- Lee JF, Stovall GM, Ellington AD. Aptamer therapeutics advance. *Curr Opin Chem Biol* 2006;10:282-9.
- Dua P, Kim S, Lee DK. Nucleic acid aptamers targeting cell-surface proteins. *Methods* 2011;54:215-25.
- Shangguan D, Cao Z, Meng L, Mallikaratchy P, Sefah K, Wang H, et al. Cell-specific aptamer probes for membrane protein elucidation in cancer cells. *J Proteome Res* 2008;7:2133-9.
- Ray P, Rialon-Guevara KL, Veras E, Sullenger BA, White RR. Comparing human pancreatic cell secretomes by *in vitro* aptamer selection identifies cyclophilin B as a candidate pancreatic cancer biomarker. *J Clin Invest* 2012;122:1734-41.
- Daniels DA, Chen H, Hicke BJ, Swiderek KM, Gold L. A tenascin-C aptamer identified by tumor cell SELEX: systematic evolution of ligands by exponential enrichment. *Proc Natl Acad Sci U S A* 2003;100:15416-21.
- Mallikaratchy P, Tang Z, Kwame S, Meng L, Shangguan D, Tan W. Aptamer directly evolved from live cells recognizes membrane bound immunoglobulin heavy mu chain in Burkitt's lymphoma cells. *Mol Cell Proteomics* 2007;6:2230-8.
- Ouyang H, Mou L, Luk C, Liu N, Karaskova J, Squire J, et al. Immortal human pancreatic duct epithelial cell lines with near normal genotype and phenotype. *Am J Pathol* 2000;157:1623-31.
- Furukawa T, Duguid WP, Rosenberg L, Viallet J, Galloway DA, Tsao MS. Long-term culture and immortalization of epithelial cells from normal adult human pancreatic ducts transfected by the E6E7 gene of human papilloma virus 16. *Am J Pathol* 1996;148:1763-70.
- Kang H.S, Min H.Y.M, Kim S, Lee DK. Isolation of RNA aptamers targeting HER-2-overexpressing breast cancer cells using cell-SELEX. *Korean Chem Soc* 2009;30:1827.
- Corpet F. Multiple sequence alignment with hierarchical clustering. *Nucleic Acids Res* 1988;16:10881-90.
- Matzura O, Wennborg A. RNAdraw: an integrated program for RNA secondary structure calculation and analysis under 32-bit Microsoft Windows. *Comput Appl Biosci* 1996;12:247-9.
- Dua P, Yoo JW, Kim S, Lee DK. Modified siRNA structure with a single nucleotide bulge overcomes conventional siRNA-mediated off-target silencing. *Mol Ther* 2011;19:1676-87.
- Irizarry RA, Bolstad BM, Collin F, Cope LM, Hobbs B, Speed TP. Summaries of Affymetrix GeneChip probe level data. *Nucleic Acids Res* 2003;31:e15.
- Dennis G Jr, Sherman BT, Hosack DA, Yang J, Gao W, Lane HC, et al. DAVID: database for annotation visualization, and integrated discovery. *Genome Biol* 2003;4:P3.
- Bartlett DW, Davis ME. Effect of siRNA nuclease stability on the *in vitro* and *in vivo* kinetics of siRNA-mediated gene silencing. *Biotechnol Bioeng* 2007;97:909-21.
- Le Du MH, Stigbrand T, Taussig MJ, Menez A, Stura EA. Crystal structure of alkaline phosphatase from human placenta at 1.8 Å resolution. Implication for a substrate specificity. *J Biol Chem* 2001;276:9158-65.
- Koyama I, Hirano K, Makiya R, Stendahl U, Stigbrand T. Purification and characterisation of the placental-like alkaline phosphatase from ovarian epithelial tumours. *Br J Cancer Suppl* 1990;10:6-11.
- Watanabe T, Wada N, Chou JY. Structural and functional analysis of human germ cell alkaline phosphatase by site-specific mutagenesis. *Biochemistry* 1992;31:3051-8.

Authors' Contributions

Conception and design: P. Dua, S. Kim, Dong-ki Lee
Development of methodology: P. Dua, H.S. Kang, S. Kim, Dong-ki Lee
Acquisition of data (provided animals, acquired and managed patients, provided facilities, etc.): P. Dua, S.-M. Hong, M.-S. Tsao
Analysis and interpretation of data (e.g., statistical analysis, biostatistics, computational analysis): P. Dua, S. Kim, Dong-ki Lee
Writing, review, and/or revision of the manuscript: P. Dua, M.-S. Tsao, S. Kim, Dong-ki Lee
Administrative, technical, or material support (i.e., reporting or organizing data, constructing databases): S. Kim
Study supervision: Dong-ki Lee

Grant Support

This work was supported by the Global Research Laboratory program by Ministry of Education and Science and Technology in Korea (grant 2008-00582; Dong-ki Lee) and by Korea Ministry of Environment as "EI project" (ERL E211-41003-0007-0; Soyoun Kim).

The costs of publication of this article were defrayed in part by the payment of page charges. This article must therefore be hereby marked *advertisement* in accordance with 18 U.S.C. Section 1734 solely to indicate this fact.

Received September 25, 2012; revised November 19, 2012; accepted December 3, 2012; published OnlineFirst March 6, 2013.

30. Otto VI, Fried R, Wiederkehr F, Hanseler E. Separation of the two most closely related isoenzymes of alkaline phosphatase by two-dimensional electrophoresis. *Electrophoresis* 1995;16:1284–8.
31. Roelofs H, Manes T, Janszen T, Millan JL, Oosterhuis JW, Looijenga LH. Heterogeneity in alkaline phosphatase isozyme expression in human testicular germ cell tumours: An enzyme-/immunohistochemical and molecular analysis. *J Pathol* 1999;189:236–44.
32. Hoylaerts MF, Millan JL. Site-directed mutagenesis and epitope-mapped monoclonal antibodies define a catalytically important conformational difference between human placental and germ cell alkaline phosphatase. *Eur J Biochem* 1991;202:605–16.
33. Neumann A, Keller T, Jocham D, Doehn C. [Human placental alkaline phosphatase (hPLAP) is the most frequently elevated serum marker in testicular cancer]. *Aktuelle Urol* 2011;42:311–5.
34. Wolf JS, Chen Z, Dong G, Sunwoo JB, Bancroft CC, Capo DE, et al. IL (interleukin)-1 α promotes nuclear factor- κ B and AP-1-induced IL-8 expression, cell survival, and proliferation in head and neck squamous cell carcinomas. *Clin Cancer Res* 2001;7:1812–20.
35. Lesina M, Kurkowski MU, Ludes K, Rose-John S, Treiber M, Kloppel G, et al. Stat3/Socs3 activation by IL-6 transsignaling promotes progression of pancreatic intraepithelial neoplasia and development of pancreatic cancer. *Cancer Cell* 2011;19:456–69.
36. Haan C, Kreis S, Margue C, Behrmann I. Jaks and cytokine receptors—an intimate relationship. *Biochem Pharmacol* 2006;72:1538–46.
37. Schuler S, Diersch S, Hamacher R, Schmid RM, Saur D, Schneider G. SKP2 confers resistance of pancreatic cancer cells towards TRAIL-induced apoptosis. *Int J Oncol* 2011;38:219–25.
38. Takano Y, Kato Y, Masuda M, Ohshima Y, Okayasu I. Cyclin D2, but not cyclin D1, overexpression closely correlates with gastric cancer progression and prognosis. *J Pathol* 1999;189:194–200.
39. Masood A, Azmi AS, Mohammad RM. Small molecule inhibitors of Bcl-2 family proteins for pancreatic cancer therapy. *Cancers* 2011;3:1527–49.
40. Ochi Y, Okabe H, Inui T, Yamashiro K. [Tumor marker—present and future]. *Rinsho Byori* 1997;45:875–83.
41. Ial'chenko NA, Lagutin VD, Lavik NN, Musin II. The clinical information value of an immunoenzyme study of the tumor markers CA-19-9, CEA and AFP in cancer of the stomach, pancreas, colon and rectum. *Vopr Onkol* 1991;37:921–4.
42. Jeppsson A, Wahren B, Brehmer-Andersson E, Silfversward C, Stigbrand T, Millan JL. Eutopic expression of placental-like alkaline phosphatase in testicular tumors. *Int J Cancer* 1984;34:757–61.
43. Paiva J, Damjanov I, Lange PH, Harris H. Immunohistochemical localization of placental-like alkaline phosphatase in testis and germ-cell tumors using monoclonal antibodies. *Am J Pathol* 1983;111:156–65.
44. Stendahl U, Lindgren A, Tholander B, Makyia R, Stigbrand T. Expression of placental alkaline phosphatase in epithelial ovarian tumours. *Tumour Biol* 1989;10:126–32.
45. Millan JL, Fishman WH. Biology of human alkaline phosphatases with special reference to cancer. *Crit Rev Clin Lab Sci* 1995;32:1–39.
46. Hustinx SR, Cao D, Maitra A, Sato N, Martin ST, Sudhir D, et al. Differentially expressed genes in pancreatic ductal adenocarcinomas identified through serial analysis of gene expression. *Cancer Biol Ther* 2004;3:1254–61.
47. Nathanson L, Fishman WH. New observations on the Regan isoenzyme of alkaline phosphatase in cancer patients. *Cancer* 1971;27:1388–97.
48. Bellazi L, Mornet E, Meurice G, Pata-Merci N, De Mazancourt P, Dieudonne MN. Genome wide expression profile in human HTR-8/Svneo trophoblastic cells in response to overexpression of placental alkaline phosphatase gene. *Placenta* 2011;32:771–7.
49. Deer EL, González-Hernández J, Coursen JD, Shea JE, Ngatia J, Scaife CL, et al. Phenotype and genotype of pancreatic cancer cell lines. *Pancreas* 2010;39:425–35.
50. O'Connor MD, Kardel MD, Iosfina I, Youssef D, Lu M, Li MM, et al. Alkaline phosphatase-positive colony formation is a sensitive, specific, and quantitative indicator of undifferentiated human embryonic stem cells. *Stem Cells* 2008;26:1109–16.

Cancer Research

The Journal of Cancer Research (1916–1930) | The American Journal of Cancer (1931–1940)

Alkaline Phosphatase ALPPL-2 Is a Novel Pancreatic Carcinoma-Associated Protein

Pooja Dua, Hye Suk Kang, Seung-Mo Hong, et al.

Cancer Res 2013;73:1934-1945. Published OnlineFirst March 6, 2013.

Updated version Access the most recent version of this article at:
doi:[10.1158/0008-5472.CAN-12-3682](https://doi.org/10.1158/0008-5472.CAN-12-3682)

Supplementary Material Access the most recent supplemental material at:
<http://cancerres.aacrjournals.org/content/suppl/2012/12/31/0008-5472.CAN-12-3682.DC1>

Cited articles This article cites 50 articles, 9 of which you can access for free at:
<http://cancerres.aacrjournals.org/content/73/6/1934.full.html#ref-list-1>

Citing articles This article has been cited by 2 HighWire-hosted articles. Access the articles at:
</content/73/6/1934.full.html#related-urls>

E-mail alerts [Sign up to receive free email-alerts](#) related to this article or journal.

Reprints and Subscriptions To order reprints of this article or to subscribe to the journal, contact the AACR Publications Department at pubs@aacr.org.

Permissions To request permission to re-use all or part of this article, contact the AACR Publications Department at permissions@aacr.org.